The ultrafast ground and excited state dynamics of *cis*-hexatriene in cyclohexane

Stuart H. Pullen, Neil A. Anderson, Larry A. Walker II, and Roseanne J. Sension[a)]
Department of Chemistry, University of Michigan, Ann Arbor, Michigan 48109-1055

(Received 29 May 1997; accepted 26 June 1997)

One- and two-color kinetics have been combined with broadband ultraviolet transient absorption spectroscopy in the 265–300 nm region to elucidate the photophysics of *cis*-hexatriene in cyclohexane solvent. The lowest singlet excited state, the $2\,^1A_1$ state, is observed to have a lifetime of 200 ± 50 fs. The ground-state hexatriene is produced vibrationally hot. The excess vibrational energy permits ultrafast isomerization around the C–C single bonds in hexatriene. This results in a dynamic equilibrium of the three *cis*-hexatriene rotamers, which then relaxes multiexponentially to the room-temperature distribution in which the di-s-*trans*-Z-hexatriene form predominates. The peak of the mono-s-*trans* (cZt-HT) population is estimated to be ~50%. Vibrational cooling results in trapping of a small amount, ~8%, of cZt-HT that relaxes on a much longer time scale as the barrier to isomerization becomes important. An estimate of the absorption spectrum of cZt-HT is deduced from analysis of the spectral data at 50 ps. © *1997 American Institute of Physics.* [S0021-9606(97)00837-4]

I. INTRODUCTION

Polyenes have long been of interest to chemists, in part because of the crucial role these molecules play in many biological processes. Two prototypical examples are the primary event in vision, which involves a *cis–trans* isomerization, and the photochemical reactions of vitamin D. The study of simple polyenes allows a direct comparison to both theoretical results and the larger biological molecules. At the same time, the study of small polyenes contributes to the general understanding of the energy redistribution processes that are crucial to reaction kinetics.

Hexatriene has been of particular interest in recent years, since the $2\,^1A_1$ state of *cis*-hexatriene (Z-HT) was observed to lie $\sim 5000\ \mathrm{cm}^{-1}$ below the $1\,^1B_2$ state.[1] This confirmed a general trend in polyenes where the lowest singlet excited state has a doubly excited configuration. Resonance Raman measurements have shown that the excited-state lifetimes of the *cis*- and *trans*-isomers of hexatriene may be extremely short.[2] A recent fluorescence excitation spectrum of the $2A$ state of Z-HT has provided evidence of multiple pathways for ground-state recovery.[3] The gas phase lifetime of the $2A$ state of hexatriene has been measured to be 250–600 fs.[4,5]

While it has been recognized for many years that electron correlation plays a major role in the character of some of the polyene excited states,[6] it has only recently become possible, using *ab initio* techniques such as CASPT2, to describe them accurately.[7] It is now becoming feasible to examine in detail the nature of the polyene states in the regions of the potential energy surfaces that dictate reaction dynamics. One attractive hypothesis, arising from the work of Robb and co-workers, is that internal conversion to the ground state in hexatriene proceeds through a conical intersection,[8] thus explaining the fast population dynamics observed in many of these systems.[2,9–11]

Another attractive feature of the Z-HT system is as a complement to the ring-opening reaction of 1,3-cyclohexadiene. This photoinitiated reaction has a 0.4 quantum yield for Z-HT formation,[12] and also occurs in under a picosecond.[10,13,14] The Z-HT photoproduct is formed vibrationally hot and then relaxes on the hexatriene ground-state surface. Investigation of the cooling dynamics of Z-HT alone should also prove a useful aid in understanding the dynamics of the ring opening of cyclohexadiene.

This paper presents kinetics measurements and time-resolved spectra in the 265–300 nm region that provide insight into the condensed-phase dynamics of Z-HT in the ground and excited states.

II. EXPERIMENT

The laser system used to perform these experiments has been described in detail previously.[15] A titanium:sapphire oscillator is amplified producing a pulse train at a repetition rate of 1 kHz, with pulses of 70 fs duration, 400 μJ/pulse energy, and a central wavelength of ~800 nm.

Two different types of experiments are described in this paper. Kinetic measurements at specific probe wavelengths were made using either the third harmonic of the Ti:sapphire laser or a harmonic of the output of an optical parametric amplifier (OPA). Time-resolved spectra were recorded by generating an ultraviolet continuum probe pulse using the third harmonic. In all cases, the samples were pumped using the third harmonic at ~270 nm. Hexatriene (Aldrich H1, 258-7) was purchased as a mixture of *cis*- and *trans*-isomers and purified using the method of Hwa *et al.*[16]

A. Kinetics measurements

The experimental setup for the kinetics measurements was a standard pump–probe scheme. The output from the Ti:

a)Electronic mail: rsension@umich.edu

sapphire laser was split into two beams using a 60–40 beam splitter, and used to pump both an OPA (60%) and a frequency tripler (40%).

Optical parametric amplification was performed using the method of Yakolev *et al.*[17] Briefly, a small fraction of the input beam was used to generate a single-filament white-light continuum. The infrared portion was used as a seed pulse for mixing with the remaining 800 nm beam in a 7-mm-thick β-barium borate (BBO) crystal. Double passing the beams using a vertical offset allowed further amplification. The amplified infrared radiation was then frequency doubled to produce visible light, which was compressed to ~200 fs with an SF10 prism pair. The resulting beam had sufficient intensity to be frequency doubled again to produce a tunable ultraviolet probe source.

The pump pulses were generated using a standard frequency tripling scheme. A 300 μm BBO crystal was used to double the input laser beam. The fundamental and second harmonic were separated using dichroic mirrors, and a translation stage in the fundamental arm was used to compensate for temporal walk-off in the doubling crystal. The beams were then recombined with a second dichroic mirror, and the third harmonic was generated by sum–frequency mixing the fundamental and second harmonic in another 300 μm BBO crystal. The resulting pump beam was ~150 fs in duration with an average energy of 1 μJ/pulse.

One-color kinetics were obtained by generating the third harmonic with both beams and attenuating the weaker beam to supply the probe pulses.

B. Spectral measurements

The experimental setup used for recording time-resolved spectra is similar to that used for the kinetics measurements. The initial beam was split with a 60–40 beam splitter. The third harmonic was generated in both arms as described above. The pump pulses in this case had an average energy of ~0.5 μJ/pulse. The more powerful arm was used to generate 1.0–1.5 μJ of the third harmonic that was then tightly focused, using an $f=25$ mm lens, into a 3-mm-thick piece of sapphire (Crystal Systems). Careful alignment and efficient third-harmonic generation caused a breakdown of the spatial profile of the beam when the sapphire was placed at the focus, resulting in continuum generation. A sample spectrum of the continuum is shown in Fig. 1. The continuum had an average energy of less than 100 nJ.

In order to minimize the temporal broadening that can be devastating to high-bandwidth pulses in the ultraviolet region, no material was present in the probe arm between the sapphire and the sample cell. Collimation and focusing of the continuum were achieved by use of a pair of off-axis spherical mirrors ($f=50$ mm and $f=100$ mm, respectively). This method has the added advantage of minimizing chromatic aberrations. Zero time delay for each spectrum was set by recording a one-color kinetic scan, with the 3 mm sapphire in the probe beam, but translated a small distance from the focal point to avoid continuum generation. Following determination of time zero, the sapphire slice was translated into the focus to generate the continuum.

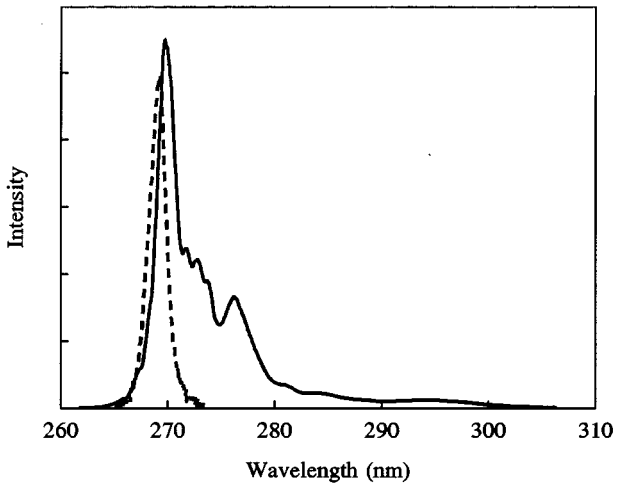

FIG. 1. Spectrum of the driving pulse used to generate ultraviolet continuum (broken line), and the resultant continuum (solid line) after focusing into a 3 mm piece of sapphire. The full width at half-maximum of the driving pulse is 1.5 nm.

The probe beam was focused onto an optical fiber, coupling the beam into a SPEX/500M monochromator with a 1200 groove/mm diffraction grating. A Princeton Instruments liquid-nitrogen-cooled charge coupled device (CCD) camera (model LN/CCD-1100-PB) was used as a detector. An overall resolution of 1 nm was achieved using this system.

Scatter from the pump beam was a major concern in these experiments. The spectra were recorded at perpendicular relative pump and probe beam polarizations so that a calcite polarizing prism placed in front of the fiber minimized detection of the pump scatter. A drawback to this method is that it complicates the interpretation of the data because of rotational contributions to the observed signal. However, this effect is expected to be small at the time delays where we have recorded spectra. The time scale for Z-hexatriene rotation in cyclohexane solution is estimated to be 4 ps, assuming slip boundary conditions. This correlates well to the reorientation time of 5.0 ps observed in the anisotropy at 290 nm (see below). Since no spectra were taken earlier than 5 ps, we have used the spectra without any correction for the difference between the magic angle and perpendicular responses.

Pumped and unpumped spectra were recorded alternately by mechanically chopping the pump beam. The CCD exposure for each spectrum was 300 ms. Difference spectra were generated by averaging the base 10 logarithm of the ratio of consecutive pumped and unpumped frames. The difference spectrum reported for each time point is an average of at least 5000 pairs of spectra.

In all of the experiments, the sample was flowed through a 1 mm path length quartz cell to allow the volume to be refreshed between laser pulses. The sample temperature was kept constant at 13.2 °C by placing the reservoir in a cooling

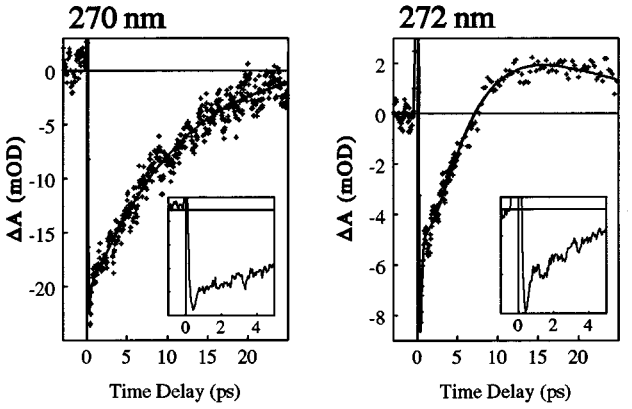

FIG. 2. One-color kinetic data for Z-hexatriene in cyclohexane. The data are magic angle at both wavelengths. Note the fast component to the bleach recovery observed at both wavelengths, and the oscillation in the early-time response at 272 nm. The solid line shows a fit of the data to a series of exponentials as described in the text.

bath, and the reservoir volume was replaced periodically to prevent sample degradation.

III. RESULTS

A. Kinetics of *cis*-hexatriene

One- and two-color pump–probe kinetic traces of *cis*-hexatriene in cyclohexane solvent are shown in Figs. 2 and 3. In all of the kinetic data, there is a solvent absorption at zero time delay due to two-photon ionization. This is only observed at zero time delay, requiring simultaneous absorption of one pump and one probe photon for ionization to occur. This artifact has been seen in all alkane solvents we have used and for all probe wavelengths below 430 nm. In pure solvent, no further kinetic signals are observed following the spike.

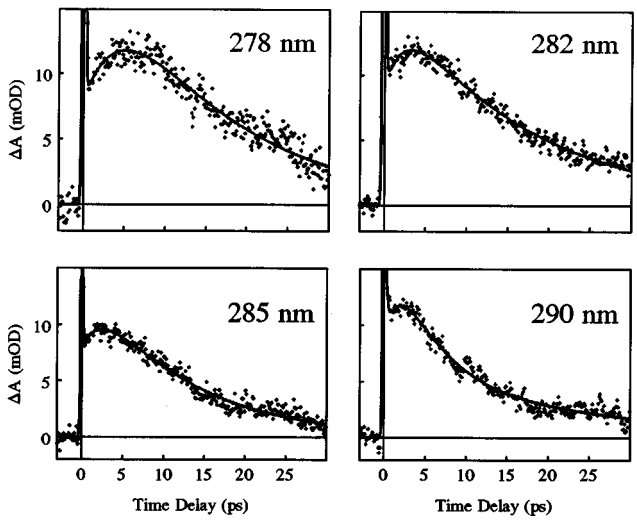

FIG. 3. Two-color kinetic data for Z-hexatriene in cyclohexane, at probe wavelengths of 278, 282, 285, and 290 nm. All data are magic angle, with an excitation wavelength of ~270 nm. The solid line shows a fit of the data to a series of exponentials as described in the text.

In the one-color kinetic measurements, the sample response is an immediate bleach followed by recovery, as a result of internal conversion to the ground state and subsequent vibrational cooling. The initial bleach in the one-color kinetic data at 272 nm appears to exhibit a coherent oscillation characteristic of impulsive excitation. This oscillation is damped within 5 ps and is not observed in any of the two-color measurements. The two-color kinetic measurements have an immediate absorption, which rises to a maximum on a varying time scale. The signal then decays as a result of both vibrational relaxation and population dynamics.

The kinetic data for all six probe wavelengths can be fit using a simple linear combination of five exponentials plus an instrument limited spike, convoluted with a Gaussian instrument response function. The width of this solvent spike allows an accurate determination of the response function. This analysis yielded two wavelength independent time constants of 200 ± 50 fs, 18 ± 2 ps, and two wavelength dependent time constants of 1–5 and 6–10 ps. A fifth time constant of 150 ps was taken from the work of Ohta and coworkers for *trans*-hexatriene (E-HT) in cyclohexane.[18] The kinetic data presented here extends only to 30 ps, so the fit is insensitive to the actual value of the long decay time constant.

The lifetime of the $1B$ state is estimated from resonance Raman spectroscopy to be ~20 fs and is too short to be observed in this data.[2] Therefore, we assign the 200 fs component to decay of the $2A$ state, leading to recovery of the ground state of hexatriene. This value is determined primarily from the fit to the one-color kinetics. The two-color kinetics have slightly worse time resolution, which occludes much of the behavior on such a short time scale. However, the appearance of transient absorption within the time resolution of the two-color kinetics provides strong additional evidence for sub-300 fs ground-state recovery. A 200 fs lifetime for the $2A$ state agrees favorably with literature values for hexatriene in the gas phase.[4,5]

In the two-color kinetics, the peak of the absorption occurs earlier as the probe wavelength moves farther red. This is caused by a decrease in the contribution to the signal by the ground-state bleach and by the broader spectrum that results from formation of a vibrationally hot ground state. Another contribution will arise if ground-state recovery leads to the formation of higher-energy rotamers of Z-HT. Although the initially excited hexatriene is in the di-s-*trans*-Z-hexatriene (tZt-HT) conformation, mono-s-*cis*-Z-HT (cZt-HT) and di-s-*cis*-Z-HT (cZc-HT) may be produced following internal conversion from the excited state. These higher-energy rotamers likely absorb to the red of tZt-HT and may account for the long-lived absorption. It is important to note that formation of E-hexatriene would not result in the small residual signal observed at 285 and 290 nm. The quantum yield for Z–E isomerization is extremely low, $<2\%$.[12] Furthermore, the absorption spectrum of the E-isomer is very

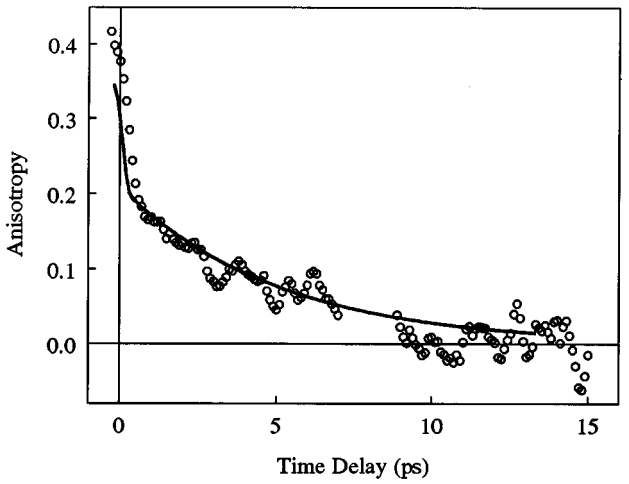

FIG. 4. The anisotropy of Z-hexatriene in cyclohexane at a probe wavelength of 290 nm. The solid line shows a fit to the data for two components, as discussed in the text. The component attributable to the observed transient absorption at this wavelength suggests an angle between pumped and probed dipoles of ~34°.

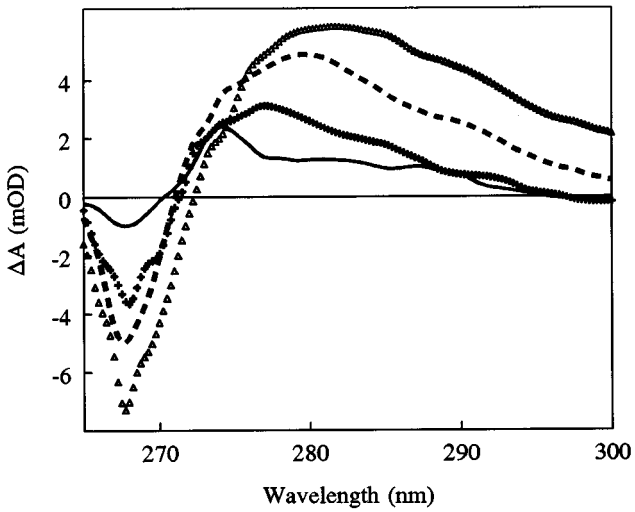

FIG. 5. Time-resolved ultraviolet spectra for Z-hexatriene recorded for various time delays (△△△ 4 ps, – – – 10 ps, +++ 20 ps, — 50 ps) after 270 nm excitation. The spectra are for perpendicular pump–probe polarization.

similar to that of Z-hexatriene, and neither isomer absorbs significantly to the red of 280 nm.

While it is possible to fit the kinetic data in Figs. 2 and 3 to a sum of exponentials, the isomerization processes that occur in this system greatly complicate the interpretation of such a fit. Many of the time constants obtained from an exponential fit to the data are not immediately assignable to individual processes. It must be recognized that cooling and isomerization are occurring simultaneously, and thus, the rates determined are a convolution of several isomerization rates together with the spectral evolution of the three conformers of Z-hexatriene. To accommodate this fact, we have included in the global analysis several intermediate time constants, but recognize that a physical model of the dynamics of this system may require several more. The effect of large amounts of vibrational energy on the ground-state dynamics of this system shall be treated in more detail in the discussion section.

The polarization dependence of the transient absorption signal at 290 nm is shown by the anisotropy plotted in Fig. 4. As will be discussed below, the signal at 290 nm is assigned primarily to the absorption of cZt-HT. The anisotropy, $r(t)$, is calculated from the transient absorption signal, obtained with parallel and perpendicular relative polarizations for the pump and probe pulses, according to Eq. (1),

$$r(t)=\frac{I_{\parallel}-I_{\perp}}{I_{\parallel}+2I_{\perp}}. \tag{1}$$

The anisotropy of the transient absorption signal from a single species is related to the average angle between the pumped and probed transition dipole moments by Eq. (2)

$$r(t)=0.4\langle P_2[\mathbf{HT}(0)\cdot\mathbf{PR}(t)]\rangle\approx r_0\ \exp(-t/\tau_r). \tag{2}$$

$\mathbf{HT}(0)$ is the transition dipole moment for *cis*-hexatriene, $\mathbf{PR}(t)$ is the transition dipole moment of the photoproduct as a function of time, and P_2 is the second Legendre polynomial. Assuming that the molecule can be approximated as a spherical diffuser, the anisotropy will decay monoexponentially from an initial value (r_0), with a time constant (τ_r) characteristic of rotational diffusion. The anisotropy shown in Fig. 4 contains contributions from two absorptions, resulting in a signal modeled according to Eq. (3)

$$r(t)=r_0^A\frac{I_A(t)}{I_A(t)+I_B(t)}+r_0^B\frac{I_B(t)}{I_A(t)+I_B(t)}\exp(-t/\tau_r). \tag{3}$$

The solvent ionization signal observed at zero time delay contributes a component with $r_0=0.40$ to the observed signal. The photoproduct component has an initial value of $r_0=0.21$ that decays with $\tau_r=5.0$ ps. Assuming a narrow distribution of angles, this value of r_0 corresponds to an angle between the pumped and probed transition dipole moment of ~34°. The difference between the transition dipoles of tZt-HT and cZt-HT is estimated to be 21° by configuration interaction calculations performed in GAUSSIAN 94,[19] arising primarily from the nonplanarity of the cZt-HT isomer. These values are in reasonable agreement considering that hexatriene is actually an asymmetric rotor and that the initial photoproduct is vibrationally excited tZt-HT, rather than cZt-HT. The cZt-HT population is built up as isomerization rapidly occurs, as will be discussed below.

B. Time-resolved spectra

Difference spectra of *cis*-hexatriene in cyclohexane solvent, after excitation at 270 nm, are shown for various time delays in Fig. 5. The spectra were smoothed using a five-point window, and then interpolation was used to remove minor features from the spectra. The continuum often had significant structure (see Fig. 1), which evolved dramatically in time. Since the pumped and unpumped frames were not

collected simultaneously, this structure could not be removed from the spectra by simple data averaging. While it is not possible to determine whether some of the structure is real, there was no distinct, reproducible fine structure in the difference spectra.

After smoothing the spectra, it was necessary to scale them to compensate for variations in signal magnitudes due to laboratory factors such as loss of overlap between pump and probe beams and fluctuations in pump energy. The kinetic data were used as a guide for this process. The absorption at each of the spectral time points was determined for each scan and the spectra were then adjusted using a scale factor and vertical offset. This process resulted in excellent agreement between kinetic and spectral data.

One concern in scaling the spectral data in this manner is the effect of the chirp on the pulse across the wavelength window. A series of spectra was taken close to zero time delay in order to characterize the chirp. Observing the two-photon solvent ionization peak at a series of time points showed that there was a nonlinear ~1 ps chirp across our spectral window. The data taken from the kinetic measurements to scale the spectra were adjusted accordingly to compensate for this minor effect.

There are two main features of note in the spectral data. First, both the bleach of the 0–0 band of the absorption spectrum and the observed absorption at longer wavelengths are seen to recover monotonically, and are approximately equal in magnitude. Second, and most important, the absorption observed at longer wavelengths is very broad, and extends out past 300 nm at the earlier time delays.

One final point of interest is that by 50 ps virtually all the bleach observed at the early time delays in the 0–0 region of the Z-HT absorption spectrum (265–272 nm) has recovered, and a small, broad residual signal is observed to the red edge of the 0–0 bleach, ~270–290 nm.

IV. DISCUSSION

A. *Cis*-hexatriene hot spectrum

The ground state of *cis*-hexatriene recovers, following optical excitation to the $1B$ state, on a ~200 fs time scale. Ground-state recovery results in significant absorption in the 280–300 nm region at early times, i.e.,<1 ps. This absorption is still present in spectra taken at 50 ps, when the bleach component has almost completely decayed. Kinetic data at 282, 285, and 290 nm clearly show the decay of this initial absorption to a small (~15%) residual absorption.

It is feasible that this red-edge absorption could be due simply to the broadening of the hexatriene absorption spectrum that results from excess vibrational energy deposited in the molecule. The exact effect of excess vibrational energy in the system is dependent on the initial amount of excess energy and the rate at which energy is lost to the bath.

The initial amount of vibrational energy in hexatriene, after excitation at 270 nm, is $37\,000 \pm 250\ \mathrm{cm}^{-1}$, depending on the precise excitation wavelength and assuming that no relaxation occurs in the excited states. The effective vibrational temperature of tZt-HT with this much excess energy may be estimated by using

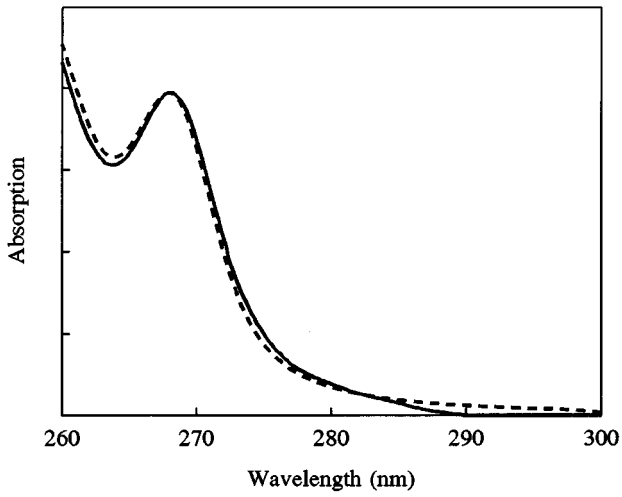

FIG. 6. Comparison of experimental (solid line) and calculated (broken line) ground-state spectra of Z-hexatriene in cyclohexane. The experimental spectrum was measured with a standard UV-VIS spectrometer. The calculated spectrum was determined using the computer program developed by the authors of Ref. 21, with parameters taken from Ref. 2.

$$\langle E_{\mathrm{RT}} \rangle + 37\,000\ \mathrm{cm}^{-1} = \sum_i h\nu_i [\exp(h\nu_i / k_B T) - 1]^{-1}, \tag{4}$$

where $\langle E_{\mathrm{RT}} \rangle$ is the average vibrational energy at room temperature and $h\nu_i$ are the harmonic frequencies for all 36 vibrations of hexatriene.[20] A temperature of ~2250 K was estimated with harmonic frequencies calculated using GAUSSIAN 94.[19] A similar temperature is obtained with experimental frequencies. The time scale for vibrational cooling in this system appears from the kinetics measurements to be in the 12–16 ps range, and an effective rate of 14 ps will be used for the discussion presented here. Assuming an exponential relaxation of the excess energy, we can then estimate that at 5 ps the equivalent temperature is approximately 1760 K, at 20 ps it is ~930 K, and at 50 ps the effective temperature is ~425 K.

Knowing this, an estimate of the effect of heating on the spectrum of the tZt-HT isomer can be made using a sum-over-states approach for independent harmonic oscillators. The algorithm used was developed by Shreve and Mathies to calculate accurate Raman excitation profiles for thermally excited molecules.[21]

Using parameters obtained from the resonance Raman studies of Ci and Myers,[2] we were able to reproduce the room-temperature absorption spectrum of *cis*-hexatriene extremely well (see Fig. 6). Hot spectra were calculated for tZt-HT at several molecular temperatures: 300, 400, 500, 750, 1000, 1500, and 2000 K. Difference spectra were generated for comparison to the experimental data by subtracting the calculated spectrum at 300 K from that at the elevated temperature. The results of these calculations for several temperatures are shown in Fig. 7. In all cases, the

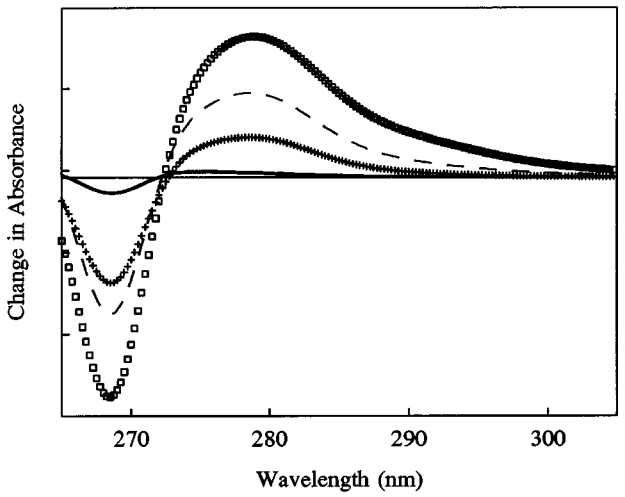

FIG. 7. Difference spectra calculated for thermal broadening of the Z-hexatriene spectrum outlined in the text. The temperatures shown are 1500 K (□□□), 1000 K (– – –), 750 K (+++), and 400 K (—).

vibrational modes used in the calculations were set at the same temperature. That is, no investigation was made of the effects of any selective vibrational excitation of the contributing modes. Also, any effect of anharmonicity is ignored in this treatment.

From comparison of the calculated difference spectra to the data, it is immediately apparent that the spectral shape of the absorption is different. The magnitude of the absorption seen to the red of 280 nm, especially at the earlier time delays, cannot be accounted for by the hot spectrum of tZt-hexatriene alone regardless of the exact rate of vibrational cooling. Clearly, vibrational excitation alone cannot explain the experimental data.

B. Single bond isomerization dynamics

The amount of vibrational energy present in the hexatriene molecule following electronic relaxation is far in excess of any barrier for single-bond isomerization. Carreira estimated a 2504 cm^{-1} barrier for s-*trans* to s-*cis* isomerization in butadiene from Raman overtones.[22] Ackerman and Kohler used low-temperature fluorescence to determine a barrier for single-bond isomerization in all-*trans*-octatetraene of 16.7 kJ/mol (1400 cm^{-1}).[23] These values suggest that single-bond isomerization in hexatriene should occur easily, and frequently, given that hexatriene returns to the ground state with over 30 000 cm^{-1} of excess vibrational energy.

To provide an estimate of the barrier for s-*trans* to s-*cis* isomerization in Z-hexatriene, transition-state calculations have been performed in GAUSSIAN 94,[19] using a restricted Hartree–Fock method with a 6-31 G basis set. The results of these calculations are summarized in Table I. Our values for the properties of the rotamers are in excellent agreement with previous calculations.[24–26] Compared to the isomerization barriers determined for butadiene and octatetraene, the barriers for isomerization in Z-HT appear somewhat low. However, barriers calculated for E-HT in the same manner are in excellent agreement with the expected trend. The lower values reported here are most likely a result of nonplanarity in the higher-energy rotamers of Z-HT.

TABLE I. Geometrical parameters and relative energies for the three rotamers of Z-hexatriene and two transition states for isomerization around a C–C single bond. The absolute energy for tZt-HT was −231.722 42 hartrees.

	tZt	tZt/cZt TS	cZt	cZt/cZc TS	cZc
Relative Energy					
(cm^{-1})	0	1809	1088	3370	2956
(kJ/mol)	0	21.64	13.02	40.31	35.36
Bond length (Å)					
$C_1=C_2$	1.338	1.318	1.323	1.318	1.320
$C_2–C_3$	1.470	1.481	1.461	1.484	1.474
$C_3=C_3'$	1.344	1.327	1.330	1.321	1.327
$C_3'–C_2'$	1.470	1.470	1.461	1.484	1.474
$C_2'=C_1'$	1.338	1.323	1.323	1.318	1.320
Bond angle (°)					
$C_1C_2C_3$	123.4	124.7	123.6	124.5	126.3
$C_2C_3C_2'$	126.8	128.1	127.2	125.4	129.5
$C_3C_3'C_2'$	126.8	130.1	128.0	125.4	129.5
$C_3'C_2'C_1'$	123.4	128.7	126.3	124.5	126.3
Dihedral angle (°)					
$C_1C_2C_3C_3'$	180.0	−95.6	−174.0	−94.4	−47.7
$C_2C_3C_3'C_2'$	0.0	−0.2	3.5	0.4	−4.5
$C_3C_3'C_2'C_1'$	180.0	−15.1	46.4	−94.4	−47.7

By calculating vibrational frequencies for the reactant and transition-state species together with the barriers described above, one can calculate rate constants for isomerization using the Whitten–Rabinovitch extension to Rice–Ramsperger–Kassel–Marcus (RRKM) theory.[27] With excess vibrational energy in the range of 25 000–30 000 cm^{-1}, the predicted rates for interconversion among the three rotamers range from $(0.3\ ps)^{-1}$ for the cZc-HT to cZt-HT isomerization, to $(0.9\ ps)^{-1}$ for the cZt-HT to cZc-HT isomerization. The rates are energy dependent, and rates for interconversion among the three rotamers at several vibrational energies are displayed in Table II.

The rates calculated in this manner admittedly ignore the effect of solvent reorganization and stabilization of reactant, product, or transition state. This approach also neglects any external friction effects on the reaction coordinate. A more important caveat to this approach is that the RRKM theory

TABLE II. RRKM rates for isomerization using the reactant and transition-state vibrations for the geometries described in Table I. The rates all have units of ps^{-1}.

E_{vib} (cm^{-1})	cZc→cZt	cZt→cZc	cZt→tZt	tZt→cZt
30 000	3.27	1.22	1.98	2.86
25 000	3.11	0.980	1.85	2.43
20 000	2.89	0.725	1.69	1.94
15 000	2.58	0.469	1.49	1.42
10 000	2.10	0.230	1.22	0.859
5000	0.976	0.0451	0.792	0.313

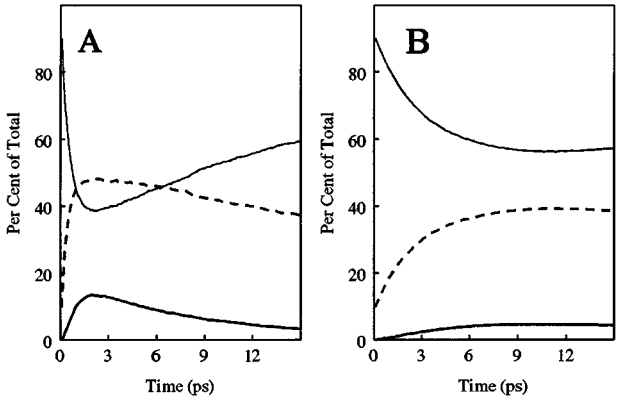

FIG. 8. Population dynamics for the rotamers of Z-hexatriene calculated using the algorithm described in Ref. 28, assuming RRKM isomerization rates, an initial 15% population of cZt-HT upon ground-state recovery, and an exponential vibrational cooling rate of 14 ps. (A) Assuming a factor of 2 reduction in all isomerization rates due to IVR and solvent effects. (B) Assuming a factor of 20 reduction in all isomerization rates due to IVR and solvent effects. The population of tZt-HT is shown by the upper solid curve, cZt-HT is shown by the broken line, and cZc-HT is the lower solid line. It is important to note from this figure that slower isomerization rates do not prevent equilibration, rather they result in a longer lifetime for the cZt-HT rotomer.

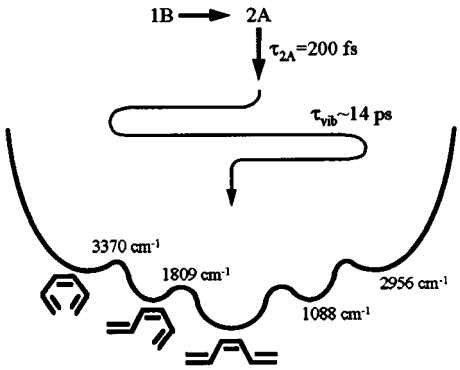

FIG. 9. The ground- and excited-state dynamics of Z-hexatriene are shown schematically with internal conversion from both excited states, leading to ground-state recovery in under 300 fs. This results in vibrational excitation in the ground state, permitting C–C single-bond isomerization among the three rotamers as the system cools. The ground-state potential well depicts the double degeneracy and relative energies of the cZc-HT and cZt-HT rotamers, together with relative energies for the transition states.

requires randomization of the vibrational energy, and we cannot assume *a priori* that this randomization is faster than vibrational cooling.[20] The simplicity and ease of implementation, however, make this an excellent first approximation.

In the limit that IVR occurs sufficiently fast, the RRKM rate for this type of single-bond isomerization should be at least in qualitative agreement with the actual value. Moreover, even if the error is substantial, the analysis suggests the rotamers still interconvert on a picosecond time scale. This is important for two reasons. First, the ultrafast interconversion in the absence of any barrier will result in the establishment of a quasiequilibrium among the three rotamers. Second, this quasiequilibrium is dynamic in that the distribution of the three rotamers is altered as a result of cooling, which dramatically affects the relative rates for isomerization. It is important to note that cooling would have to occur much faster than isomerization, and thus at a rate inconsistent with the data, in order to prevent this equilibration process.

This equilibration allows us to postulate that the excess absorption in the 280–300 nm region is the result of the rapid formation of a substantial population of cZt-HT. The initial equilibrium may produce as much as 50% cZt-HT. The distribution of the three rotamers can be modeled analytically as a function of time, using a reaction probability method such as that developed by Gillespie.[28] The time dependence of the distribution is shown in Fig. 8. The most consistent description of the kinetics of Z-hexatriene following excitation is then cartooned in Fig. 9.

The calculated hot tZt-HT spectra predict that this species cannot account for most of the absorption observed in the 285–300 nm region. Therefore, this component of our signal must correspond to the rapid appearance of higher-energy rotamers of Z-HT. Analysis of the kinetic and spectral data suggests that the initial recovery of the ground state leads to the equilibration of the three rotamers of Z-HT, on a ~1–3 ps time scale, and certainly within 5 ps. The equilibrium composition then evolves, as cooling occurs with a longer ~14 ps time constant. The slower signal decay at intermediate times is, thus, a result of spectral evolution and the change in distribution of the rotamers as the relative rate constants change with vibrational relaxation. The RRKM rates predict a peak in the cZt-HT population of ~50%, dropping to about 15% in ~3 vibrational cooling time periods. After significant vibrational cooling has occurred, some of the population of cZt-HT becomes trapped in the potential well, and isomerization to tZt-HT occurs on a much longer time scale. Our calculations suggest this barrier-crossing process may occur on a >200 ps time scale at 300 K. This slow rate is in reasonable agreement with values observed in the study of cyclohexadiene by Reid *et al.*,[9] and for E-hexatriene in cyclohexane by Ohta *et al.*[18]

The final point of interest with this approach to the dynamics of hot hexatriene is that the initial distribution of rotamers upon ground-state recovery may have only a minor effect on the observed behavior. The C–C single-bond isomerization rates following ground-state recovery are fast enough that equilibration would result from any initial composition. For example, excitation of tZt-HT results in the formation of vibrationally excited tZt-HT, which then isomerizes as discussed to produce populations of cZc- and cZt-HT. We could investigate the dynamics of Z-HT following ground-state recovery to the cZc-HT form, as would be the case in the ring-opening reaction of 1,3-cyclohexadiene.[9,12–15] The equilibration process that follows should result in essentially the same behavior within a few picoseconds, since the relative populations of the three conformers will depend only on the ratios of the rates for isomerization between them. This interesting facet of the ground-state dynamics of hexatriene will be investigated further in a future publication.

C. The spectrum of cZt-HT

There is little experimental data available regarding the absorption spectra of the less stable rotamers of *cis*-hexatriene. However, studies of analogues are able to provide some insight into this question. Brouwer and coworkers have studied the photochemistry of methyl- and *t*-butyl-derivatives of hexatriene in some detail, using steric hindrance to lock the conformation of the single bonds into a cZc- or cZt-HT form.[29] Circular dichroism has also been used by Matuszewski *et al.* on hexalins to elucidate the absorption spectrum of the cZc rotamer.[30] Both of these studies strongly indicate that the less stable rotamers have a spectrum that is redshifted and broadened from tZt-HT.

An absorption spectrum of E-HT has been recorded by Furikawa *et al.*, containing a significant percentage of the cEt form. Irradiated vapor from a jet expansion was deposited onto a solid substrate, thereby ''freezing'' the dynamics of the rotamers. This resulted in a significant increase in the absorption on the red edge of the tEt-HT spectrum, i.e., from 260–300 nm.[26] The spectrum also contained a contribution from cEc-HT. Unfortunately, no attempt was made to determine the magnitude of these contributions or to deduce absorption spectra for cEc-HT or cEt-HT. However, the data do provide strong evidence of cEt-HT absorption in the 260–290 nm region. Since the steady-state absorption spectra of Z- and E-HT do not differ significantly,[31] it is reasonable to expect that cZt-HT and cEt-HT also absorb in a similar spectral region. From the data available, it seems reasonable to assume that the spectrum of cZt-HT will be redshifted and broadened from that of tZt-HT. The ratio of oscillator strengths for the two rotamers is experimentally unknown, but theoretical calculations indicate that the oscillator strength of cZt-HT is roughly half as strong as that of tZt-HT.[10]

It is possible to deduce the absorption spectrum of cZt-HT from the experimental spectrum recorded at a time delay of 50 ps. One complication to the analysis of the 50 ps spectrum is that the tZt-HT spectrum has still not completely relaxed vibrationally, having an effective molecular temperature of ~400 K. This effect can easily be handled by using the calculated hot spectrum for 400 K generated above.

Another complication to the analysis of the 50 ps spectrum is the possibility of perturbation from the presence of cZc-HT. Even if a significant population of cZc-HT was formed in the initial equilibrium, this population will have declined substantially by 50 ps. The thermal activation time constants are still on the order of 5–10 ps for rotational isomerization of cZc-HT to cZt-HT. Any small population that might become ''trapped'' in the cZc-HT potential well will decay to negligible levels by 50 ps.

Now the cZt spectrum can be generated by applying Eq. (5) to each wavelength in our spectral window.

$$(N_{\mathrm{cZt}})(A_{\mathrm{cZt}}) = A_{300\ \mathrm{K}} + \mathrm{DATA}_{50\ \mathrm{ps}} - (1 - N_{\mathrm{cZt}})(A_{400\ \mathrm{K}}). \tag{5}$$

N_{cZt} refers to the fraction of cZt-HT present at 50 ps, which we estimate to be ~10%. $A_{300\ \mathrm{K}}$ and $A_{400\ \mathrm{K}}$ are the absorptions of tZt-HT calculated at 300 and 400 K, respectively, using the method described above. $\mathrm{DATA}_{50\ \mathrm{ps}}$ refers to the experimental data from the 50 ps difference spectrum. Solving Eq. (5) for A_{cZt} produces the cZt-HT spectrum shown in Fig. 10.

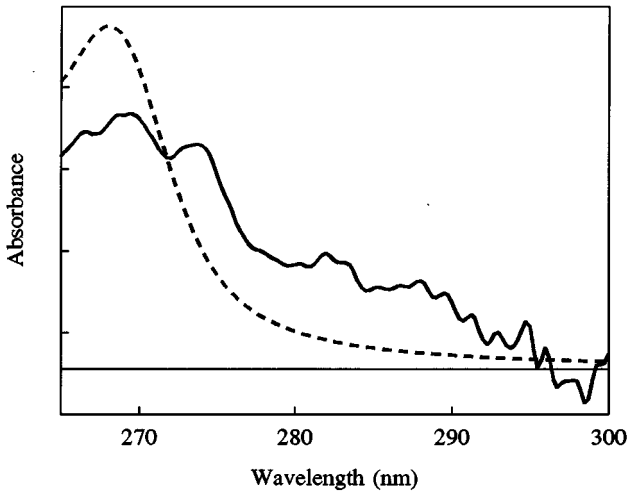

FIG. 10. Comparison of the spectrum of tZt-HT (dashed line) to the estimated spectrum of cZt-HT (solid line) determined from the transient spectrum observed at 50 ps.

As a test of the validity of these results, we have modeled early time spectra with a combination of the corresponding calculated hot spectrum and the estimated cZt-HT spectrum. These results are shown in Fig. 11. The 10 ps spectrum is in good agreement with a combination of the 1200 K tZt-HT hot spectrum (70%) and the estimated cZt-HT spectrum (30%). Moreover, the 20 ps spectrum is excellently reproduced by a 750 K tZt-HT spectrum (85%) and the estimated cZt-HT spectrum (15%).

It is interesting that the 5 ps spectrum is not reproduced well by a 1500 K hot spectrum together with the cZt-HT estimated spectrum. This is not surprising at this early time

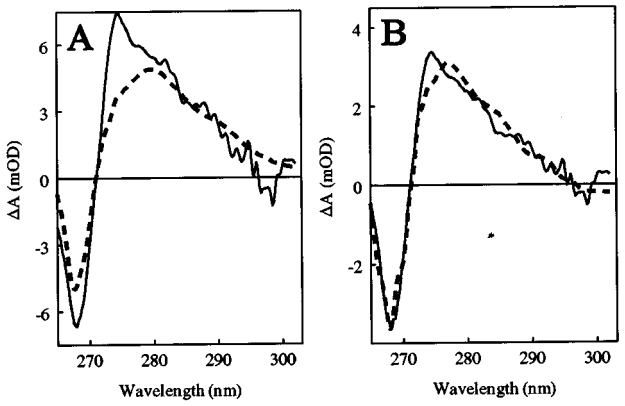

FIG. 11. Comparison of experimental (dashed line) difference spectra observed at (A) 10 ps and (B) 20 ps, with calculated spectra (solid line). The calculated spectra were produced from a combination of the estimated cZt-HT spectrum and a hot spectrum generated at the relevant temperature for a 10 ps (1000 K) or 20 ps (750 K) time delay.

delay because of the higher percentage of cZc-HT expected to be present here. Also, at 5 ps, the cZt-HT spectrum may be broadened substantially as a result of vibrational excitation.

V. CONCLUSION

This paper presents an analysis of the dynamics of *cis*-hexatriene in cyclohexane solution, in both the ground and excited electronic states. The data demonstrate that the lifetime of the $2\,^1A_1$ state is approximately 200 fs. Following internal conversion back to the ground state, significant carbon–carbon single-bond isomerization occurs. The vibrational excitation resulting from ground-state recovery allows interconversion among the three rotamers of Z-HT on a $\sim$1–3 ps time scale. This rapidly produces an equilibrium of the three rotamers, which then evolves in composition as vibrational cooling progresses. Finally, cooling results in a trapping of $\sim$8% cZt-HT. Isomerization to the more energetically favorable tZt-HT then occurs on a much longer ($\gg$100 ps) time scale, as the barrier to isomerization is encountered and activation is required for isomerization. This ''trapping'' effect has allowed us to estimate an absorption spectrum for cZt-HT.

One would expect that both the initial form of HT and the solvent would play an important role in the precise behavior of this system. Work is in progress to study, among other issues, the result of initiating ground-state dynamics with cZc-HT, following ultraviolet excitation of 1,3-cyclohexadiene. The effect of increased solvent viscosity may also result in a different trapping yield for cZt-HT, and would help elucidate solvent effects on the ground-state dynamics of hexatriene.

ACKNOWLEDGMENTS

The authors would like to thank the following: Professor Arthur J. Ashe III for his gracious donation of time, equipment, and laboratory space in the purification of the hexatriene isomers; A.-C. Tien and T. S. Sosnowski at the Center for Ultrafast Optical Science for discussion and assistance with the optimization of the generation of pump and probe pulses; Professor J. R. Barker for useful discussion regarding the application of the RRKM theory; and Dr. A. P. Shreve for the code to calculate the hot spectra. This work was supported by a grant from the National Science Foundation (No. CHE-9415772). One of the authors (S.H.P.) is supported by the NSF through the Center for Ultrafast Optical Science, under NSF Grant No. STC PHY 8920108.

[1] W. J. Buma, B. E. Kohler, and K. Song, J. Chem. Phys. **94**, 6367 (1991).
[2] X. Ci and A. B. Myers, J. Chem. Phys. **96**, 6433 (1992); A. B. Myers and K. S. Pranata, J. Phys. Chem. **93**, 5079 (1989).
[3] H. Petek, A. J. Bell, R. L. Christensen, and K. Yoshihara, J. Chem. Phys. **96**, 2412 (1992).
[4] C. C. Hayden and D. W. Chandler, J. Phys. Chem. **99**, 7897 (1995).
[5] W. Fuß, T. Schikarski, W. E. Schmid, S. Trushin, K. L. Kompa, and P. Hering, J. Chem. Phys. **106**, 2205 (1997).
[6] K. Schulten and M. Karplus, Chem. Phys. Lett. **14**, 305 (1972).
[7] K. Andersson, P. A. Malmqvist, and B. O. Roos, J. Chem. Phys **96**, 1218 (1992); B. O. Roos, K. Andersson, and M. P. Fülscher, Chem. Phys. Lett. **192**, 5 (1992); L. Serrano-Andres, B. O. Roos, and M. Merchan, Theor. Chim. Acta **87**, 387 (1994).
[8] M. Olivucci, F. Bernadi, P. Celani, I. Ragazos, and M. A. Robb, J. Am. Chem. Soc. **116**, 1077 (1994).
[9] P. J. Reid, S. J. Doig, S. D. Wickham, and R. A. Mathies, J. Am. Chem. Soc. **115**, 4754 (1993).
[10] S. Pullen, L. A. Walker II, B. Donovan, and R. J. Sension, Chem. Phys. Lett. **242**, 415 (1995).
[11] P. J. Reid, S. J. Doig, and R. A. Mathies, J. Phys. Chem. **94**, 8396 (1990); M. O. Trulson, G. D. Dollinger, and R. A. Mathies, J. Chem. Phys. **90**, 4274 (1989).
[12] H. J. C. Jacobs and E. Havinga, Adv. Photochem. **11**, 305 (1979).
[13] S. H. Pullen, L. A. Walker II, N. A. Anderson, and R. J. Sension, in *Ultrafast Phenomena X*, edited by P. Barbara, J. G. Fujimoto, W. Knox, and W. Zinth (Springer, Berlin, 1996), p. 266.
[14] W. Fuß, S. Lochbrunner, W. E. Schmid, and K. L. Kompa, in *Ultrafast Phenomena X*, edited by P. Barbara, J. G. Fujimoto, W. Knox, and W. Zinth (Springer, Berlin, 1996), p. 260; W. Fuß, T. Schikarski, W. E. Schmid, S. Trushin, and K. L. Kompa, Chem. Phys. Lett. **262**, 675 (1996); S. A. Trushin, W. Fuß, T. Schikarski, W. E. Schmid, and K. L. Kompa, J. Chem. Phys. **106**, 9386 (1997).
[15] S. Pullen, L. A. Walker II, and R. J. Sension, J. Chem. Phys. **103**, 7877 (1995).
[16] J. C. H. Hwa, P. L. de Benneville, and H. J. Sims, J. Am. Chem. Soc. **82**, 2537 (1960).
[17] V. V. Yakolev, B. Kohler, and K. R. Wilson, Opt. Lett. **19**, 2000 (1994).
[18] K. Ohta, Y. Naitoh, K. Tominaga, N. Hirota, and K. Yoshihara, *Ultrafast Phenomena X*, edited by P. Barbara, J. G. Fujimoto, W. Knox, and W. Zinth (Springer, Berlin, 1996), p. 260; K. Ohta, Y. Naitoh, K. Saitow, K. Tominaga, N. Hirota, and K. Yoshihara, Chem. Phys. Lett. **256**, 629 (1996).
[19] M. J. Frisch, G. W. Trucks, H. B. Schlegel, P. M. W. Gill, B. G. Johnson, M. A. Robb, J. R. Cheeseman, T. Keith, G. A. Petersson, J. A. Montgomery, K. Raghavachari, M. A. Al-Laham, V. G. Zakrzewski, J. V. Ortiz, J. B. Foresman, C. Y. Peng, P. Y. Ayala, W. Chen, M. W. Wong, J. L. Andres, E. S. Replogle, R. Gomperts, R. L. Martin, D. J. Fox, J. S. Binkley, D. J. Defrees, J. Baker, J. P. Stewart, M. Head-Gordon, C. Gonzalez, and J. A. Pople, GAUSSIAN 94, Revision B. 3, Gaussian, Inc., Pittsburgh, PA, 1995.
[20] R. J. Sension, S. T. Repinec, A. Z. Szarka, and R. M. Hochstrasser, J. Chem. Phys. **98**, 6291 (1993), especially Ref. 48.
[21] A. P. Shreve and R. A. Mathies, J. Phys. Chem. **99**, 7285 (1995).
[22] L. A. Carreira, J. Chem. Phys. **62**, 3851 (1975).
[23] J. R. Ackerman and B. E. Kohler, J. Chem. Phys. **80**, 45 (1984).
[24] Y. N. Panchenko, V. Kranoshchiokov, P. George, and C. W. Bock, Struct. Chem. **3**, 15 (1992).
[25] R. Liu and X. Zhou, J. Phys. Chem. **97**, 1850 (1993).
[26] Y. Furukawa, H. Takeuchi, I. Harada, and M. Tasumi, J. Mol. Struct. **100**, 341 (1983); H. Yoshida, Y. Furukawa, and M. Tasumi, *ibid*. **194**, 279 (1989).
[27] *Unimolecular Reactions*, 2nd ed., edited by K. A. Holbrook, M. J. Pilling, and S. H. Robertson (Wiley, New York, 1996), and references contained therein; G. Z. Whitten and B. S. Rabinovitch, J. Chem. Phys. **41**, 1883 (1964); D. C. Tardy, B. S. Rabinovitch, and G. Z. Whitten, *ibid*. **48**, 1427 (1968).
[28] D. T. Gillespie, J. Comp. Phys. **22**, 403 (1976).
[29] A. M. Brouwer, J. Cornelisse, and H. J. C. Jacobs, J. Photochem. Photobiol. A **42**, 117 (1988); Tetrahedron **43**, 435 (1987).
[30] B. Matuszewski, A. W. Burgstahler, and R. S. Givens, J. Am. Chem. Soc. **104**, 6874 (1982).
[31] N. G. Minnaard and E. Havinga, Recueil **92**, 1179 (1973); R. M. Gavin, Jr., S. Riesenberg, and S. A. Rice, J. Chem. Phys. **58**, 3160 (1973).